0888-8809/06/$15.00/0
Printed in U.S.A.

Molecular Endocrinology 20(7):1610–1622

doi: 10.1210/me.2005-0494

Fat Aussie—A New Alström Syndrome Mouse Showing a Critical Role for ALMS1 in Obesity, Diabetes, and Spermatogenesis

Todor Arsov, Diego G. Silva, Moira K. O'Bryan, Amanda Sainsbury, Nicola J. Lee, Claire Kennedy, Shehnaaz S.M. Manji, Keats Nelms, Conan Liu, Carola G. Vinuesa, David M. de Kretser, Christopher C. Goodnow,* and Nikolai Petrovsky*

John Curtin School of Medical Research (T.A., D.G.S., C.G.V., C.C.G.), The Australian National University, and The Canberra Hospital and The Australian National University Medical School (T.A., D.G.S.), Canberra ACT 2601, Australia; Monash Institute of Medical Research and The Australian Research Council Centre of Excellence in Biotechnology and Development (M.K.O., C.K., D.M.d.K.), Monash University, Melbourne, Victoria 3168. Australia; Garvan Institute of Medical Research (A.S., N.J.L.), Sydney, New South Wales 2010, Australia; Murdoch Childrens Research Institute (S.S.M.M.), Royal Children's Hospital, Melbourne, Victoria 3052, Australia; Phenomix Australia Pty Ltd (K.N., C.L.), and The Australian Phenomics Facility (C.C.G.), Canberra ACT 2601, Australia; and Flinders Medical Centre and Flinders University (N.P.), Bedford Park, Adelaide, South Australia 5042, Australia

Mutations in the human ALMS1 gene are responsible for Alström syndrome, a disorder in which key metabolic and endocrinological features include childhood-onset obesity, metabolic syndrome, and diabetes, as well as infertility. ALMS1 localizes to the basal bodies of cilia and plays a role in intracellular trafficking, but the biological functions of ALMS1 and how these relate to the pathogenesis of obesity, diabetes, and infertility remain unclear. Here we describe a new mouse model of Alström syndrome, *fat aussie,* caused by a spontaneous mutation in the *Alms1* gene. *Fat aussie* (*Alms1 foz/foz*) mice are of normal weight when young but, by 120 d of age, they become obese and hyperinsulinemic. Diabetes develops in *Alms1 foz/foz* mice accompanied by pancreatic islet hyperplasia and islet cysts. Female mice are fertile before the onset of obesity and metabolic syndrome; however, male *fat aussie* mice are sterile due to a progressive germ cell loss followed by an almost complete block of development at the round-to-elongating spermatid stage of spermatogenesis. In conclusion, *Alms1 foz/foz* mouse is a new animal model in which to study the pathogenesis of the metabolic and fertility defects of Alström syndrome, including the role of ALMS1 in appetite regulation, pathogenesis of the metabolic syndrome, pancreatic islet physiology, and spermatogenesis. (*Molecular Endocrinology* 20: 1610–1622, 2006)

ALSTRÖM SYNDROME [Online Mendelian Inheritance in Men (OMIM) 203800] is a rare autosomal-recessive condition. More than 300 patients have been collected in the Jackson Lab Alström syndrome database (1). This syndrome affects multiple organs and involves sensorineural hearing loss, pigmented retinal degeneration leading to blindness, obesity, glucose metabolism disturbances (insulin resistance and type 2 diabetes), and hypertriglyceridemia (1–6). In addition, some patients with Alström syndrome have hypothyroidism, low GH levels (with accelerated bone maturity, short stature, and dental abnormalities), dilated cardiomyopathy and congestive heart failure, and fatty liver disease with elevated levels of liver enzymes and/or kidney failure (1, 2, 4, 7–10). The clinical expression of the syndrome is variable, and members of the same kindred bearing the same mutation often present with different symptoms and at variable ages. However, none of the Alström syndrome patients studied have ever reproduced (1).

Two independent groups reported that mutations in human *Alms1* are responsible for this syndrome in humans (11–16). *Alms1* is a widely expressed gene that encodes a 461-kDa [4169-amino acid (aa)] protein with a largely unknown function (15, 16). It contains a large tandem repeat domain coded by a single exon 8 comprising 34 imperfect repeats of a 44-aa sequence. This domain constitutes 40% of the protein. ALMS1 also has a short polyglutamine segment (17 Glu repeats, aa 13–29), which is followed by seven alanine residues (aa 30–36). In addition to a predicted leucine zipper domain (aa 2480–2501), this protein has an evolutionary conserved motif, the Alms motif, near the C terminus. This sequence is similar to a sequence of

First Published Online March 2, 2006

* C.C.G. and N.P. contributed equally as senior authors to this paper.

Abbreviations: aa, Amino acids; BMI, body mass index; dB, decibel; DXA, dual x-ray absorptiometry; NOD, nonobese diabetic.

***Molecular Endocrinology* is published monthly by The Endocrine Society (http://www.endo-society.org), the foremost professional society serving the endocrine community.**

a predicted protein of unknown function in mouse and macaque (15, 16).

Although ALMS1 has been found to localize to centrosomes and basal bodies of cell cilia, its function remains largely unknown (17–18). Based on the clinical resemblance of Alström syndrome to the Bardet-Biedl syndrome and data showing that cilia play a sensory as well as mechanical role in several cell types, it has been hypothesized that basal body and/or ciliary dysfunction may underpin the pathogenesis of Alström syndrome (18). However, the way in which such a cellular abnormality could cause obesity is unclear. Disordered appetite regulation could be central to such a disorder, but metabolic studies in children with Alström syndrome have, to date, been inconclusive. Further, because of the complex interaction between general well-being and fertility, the nature of the reproductive abnormalities in this syndrome remains uncertain.

Recently an *Alms1* gene-trapped deleted mouse has been described (19) in which partial deletion of the mouse *Alms1* gene caused a phenotype similar to the human condition and implicated ALMS1 in intracellular trafficking. Although diabetes is a constant and serious complication in both male and female Alström syndrome patients and in the *fat aussie* mice described herein, only male *Alms1* gene-trapped mice developed moderate diabetes, and this appeared to be relatively late in onset. Although hypogonadism was reported in *Alms1* gene-trapped mice, no data were provided on their reproductive performance, testicular weight, or reproductive hormone levels (19).

Here we describe the identification and phenotypic characterization of a new mouse model of Alström syndrome, the *fat aussie* (*foz/foz*) mouse, bearing a spontaneous 11-bp deletion (*foz*) in exon 8 of the mouse *Alms1* gene. This mutation leads to a phenotype that recapitulates the human condition and demonstrates direct involvement of *Alms1* in the regulation of spermatogenesis.

RESULTS

Genetic Characterization of *Fat Aussie* (*Alms1 foz/foz*) Mice

The *fat aussie* (*foz*) strain was identified as a spontaneous recessive variant occurring in a nonobese diabetic (NOD) mouse colony, with the most conspicuous phenotypic change being obesity that became obvious by 100–120 d of age. The causative gene variant was localized in a F_2 intercross to a 3-Mbp interval on mouse chromosome 6 (between markers D6Mit8 and D6Mit29) containing 42 predicted genes. These include *Alms1* (Fig. 1A), a recently described gene that is widely expressed and disrupted by mutations in a human obesity syndrome, Alström syndrome (15, 16). Sequencing of *Alms1* cDNA from *foz/foz* liver revealed an 11-bp deletion in exon 8 at nucleotides 3918–3928, compared with the parental NOD sequence (Fig. 1, B and C). Similar to several human mutations, the *fat aussie* deletion causes a frame-shift and premature termination codon within this domain, eliminating the C-terminal two thirds of the protein (8–15). PCR using primers flanking the deletion confirmed absolute concordance between obesity and homozygosity for the deletion (Fig. 1D).

Changes in Food Intake and Body Composition in *Alms1 foz/foz* Mutant Mice

Female *Alms1 foz/foz* mice first developed a significantly increased body mass index (BMI) relative to heterozygous carriers or wild-type controls at 90 d of age. By 150 d of age they attained a BMI twice that of the controls (Fig. 2A). Similar obesity occurred in male *Alms1 foz/foz* animals (Fig. 3A). There was no significant difference in BMI between heterozygous mice and +/+ controls at any age (Figs. 2A and 3A).

Nasal-anal length was not different in the male mutant mice as compared with the heterozygotes and the normal mice at any age (data not shown). Female *Alms1 foz/foz* mice were longer than +/+ mice by 0.3–0.5 cm ($P < 0.01$; n =10 mice per group; data not shown). However, the increased BMI of *Alms1 foz/foz* mice was almost entirely accounted for by an increase in body fat. Thus dual x-ray absorptiometry (DXA) scanning demonstrated a doubling in percentage of body fat in both male and female *Alms1 foz/foz* mice from 70–90 d of age (Figs. 2C and 3C). In addition, older mice had significantly higher values for lean body weight (Figs. 2D and 3D).

Measurements of food intake in individually housed male and female mice showed that food consumption was indistinguishable in *Alms1 foz/foz* mice compared with wild-type controls at age 30 d (data not shown). However, both male and female mutant mice became hyperphagic relative to wild-type mice from 60 d of age. At age 180 d, *Alms1 foz/foz* mice ate 30–42% more than their heterozygous and wild-type littermates (Figs. 2B and 3B). Male *foz/foz* mice consumed 54 kJ/d compared with 39 kilojoules (kJ)/d for their normal siblings ($P < 0.001$; Fig. 3B), whereas the daily energy intake of female *Amls1 foz/foz* animals was 53 kJ/d compared with 40 kJ/d for controls ($P < 0.001$; Fig. 2B).

Metabolic Changes in *Fat Aussie* Mice

After the development of obesity, *Alms1 foz/foz* mice developed the characteristic features of type 2 diabetes. Fed with a normal diet, one of eight *Alms1 foz/foz* males became hyperglycemic by age 75 d (defined as having a fasting blood glucose concentration greater than 10 mmol/liter and glycosuria, with an average glycemia of 10.4 mmol/liter), four of eight were diabetic by age 90 d (range of glycemia 10.1–18.4 mmol/liter), six of eight were diabetic by age 135 d (range of glycemia 14.6–36.2 mmol/liter), and all were diabetic with glucose levels above 10

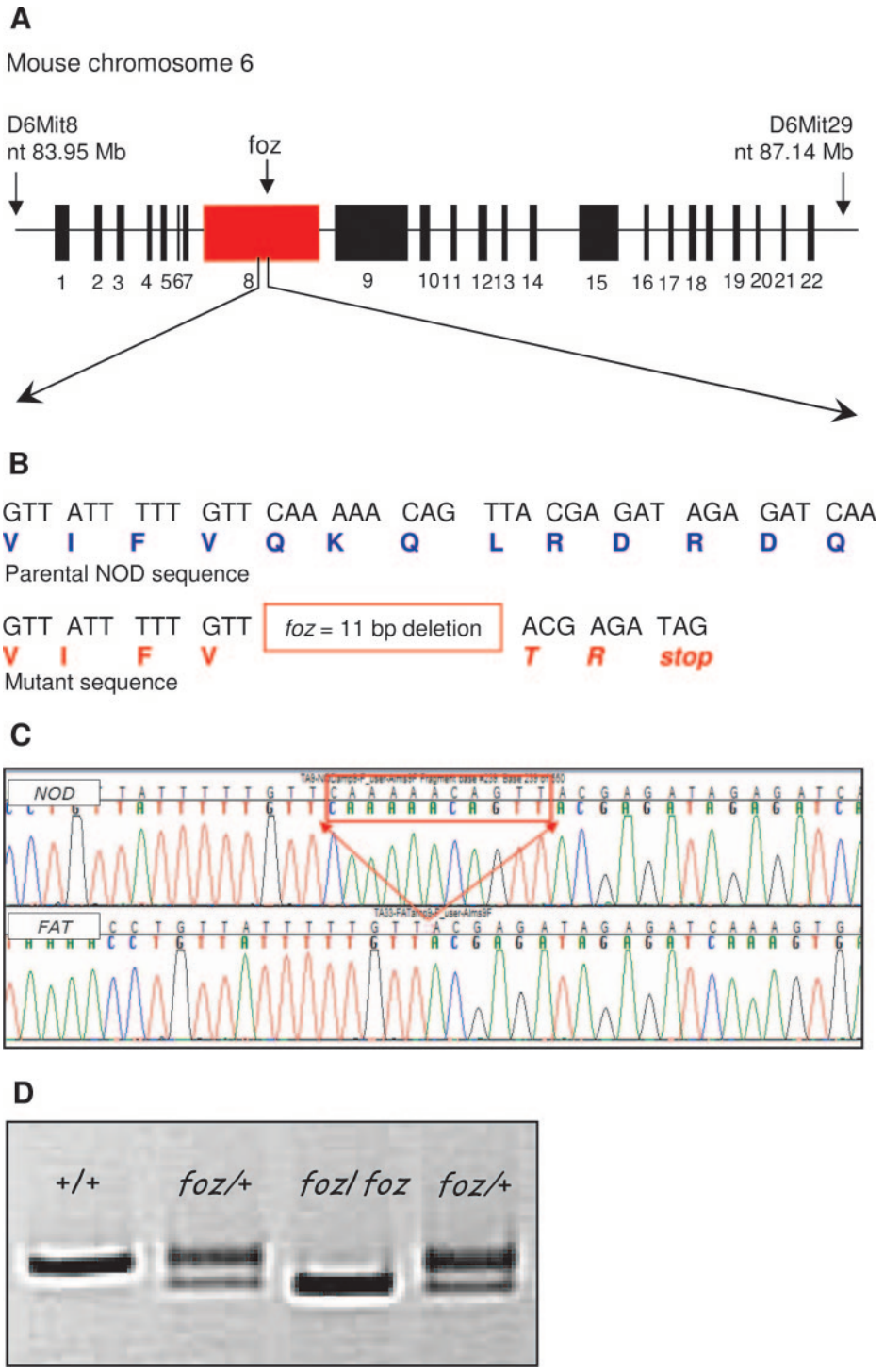

Fig. 1. *Fat Aussie* Inherits an 11-bp Deletion in *Alms1* Exon 8 Creating a Frameshift and Premature Stop Codon

A, Mouse *Alms1* gene structure. B and C, Sequence of normal and mutant (*foz/foz Alms1*) cDNA showing 11-bp deletion (nt 3918–3928) in exon 8 (between *arrows*). Normal protein (in *blue*) and truncated protein (in *red*) sequences are given *below* the normal and mutant nucleotide sequence. D, Gel photoreproduction (4% agarose gel) showing PCR results for the +/+, *foz*/+, and *foz/foz* genotypes. Nt, Nucleotide; Mb, megabases.

mmol/liter and glycosuria by 150 d of age. None of the heterozygotes and +/+ siblings developed hyperglycemia or glycosuria (Fig. 5A). Female *Alms1 foz/foz* developed diabetes slightly later: one of 11 was diabetic by age 105 d (with an average glycemia of 10.4 mmol/liter), nine of 11 were diabetic by age 120 d (range of glycemia, 12.1–18.6 mmol/liter), and nine of 11 were diabetic by age 135 d (range of

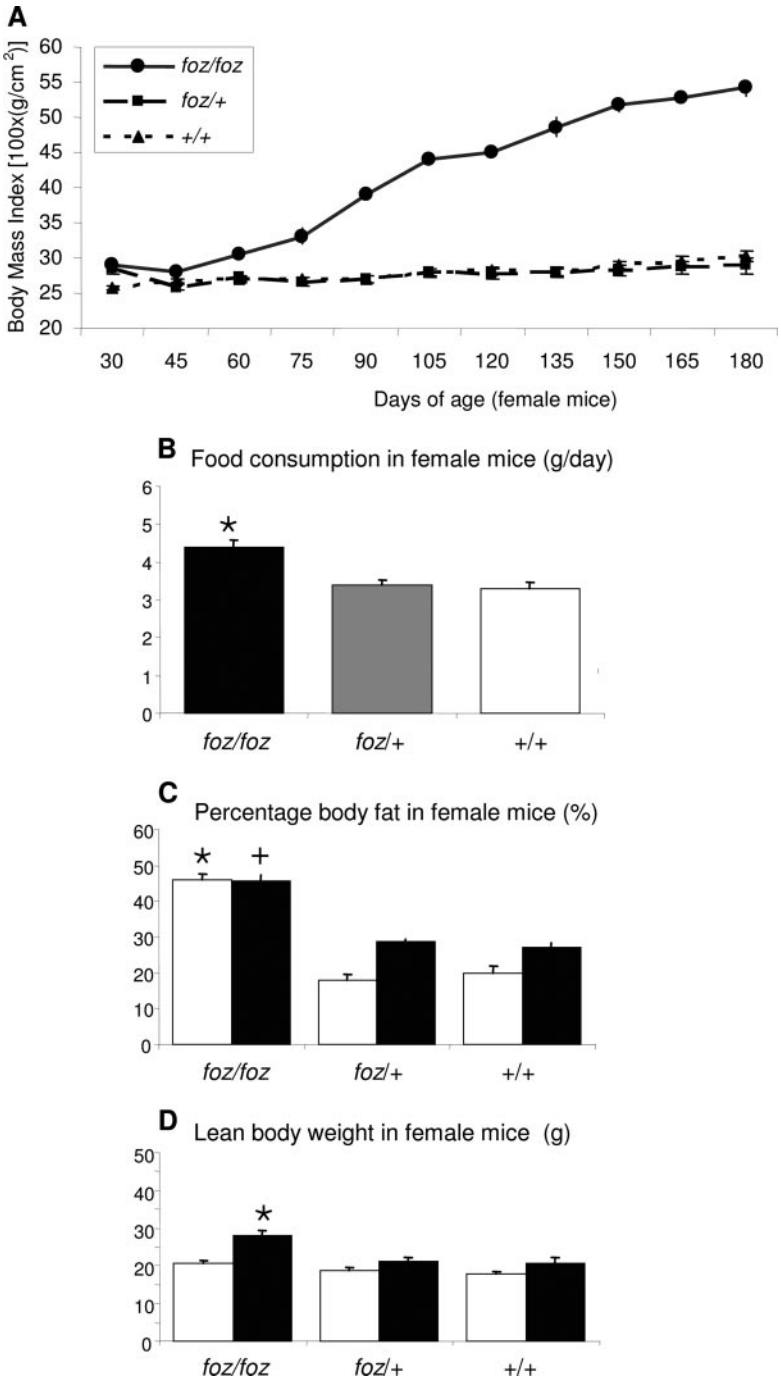

Fig. 2. Effect of Genotype on BMI, Food Consumption, and Body Composition in Female Mice

A, BMI growth curves for female mice of each genotype (n = 10–12 per group). B, Increased food consumption in female mice (age 180 d, n = 6 per group; individually housed mice, mean values from food consumption in 3 consecutive days). *Alms1 foz/foz* consumed significantly more food than *foz*/+ and +/+ control mice (*, $P < 0.01$). C, Percentage of body fat measured by DXA scanning. Both young (70 d old, *white bars*) and old (250 d old, *black bars*) *Alms1 foz/foz* mice have significantly higher percentage of body fat compared with *foz*/+ and +/+ controls (*, $P < 0.001$; +, $P < 0.05$). D, Lean body weight analysis shows no significant difference between the three genotypes at a younger age (70 d old, *white bars*). Only older (250 d old, *black bars*) female *Alms1 foz/foz* mice have significantly higher lean body weight compared with *foz*/+ and +/+ (*, $P < 0.001$) control mice.

glycemia, 10.5–23.2 mmol/liter) (Fig. 5B). Before developing overt hyperglycemia, *Alms1* mutant (*foz/foz*) mice were glucose intolerant as judged by the delayed peak of glycemia and longer time needed to return to baseline levels after ip administration of glucose (Fig. 5A).

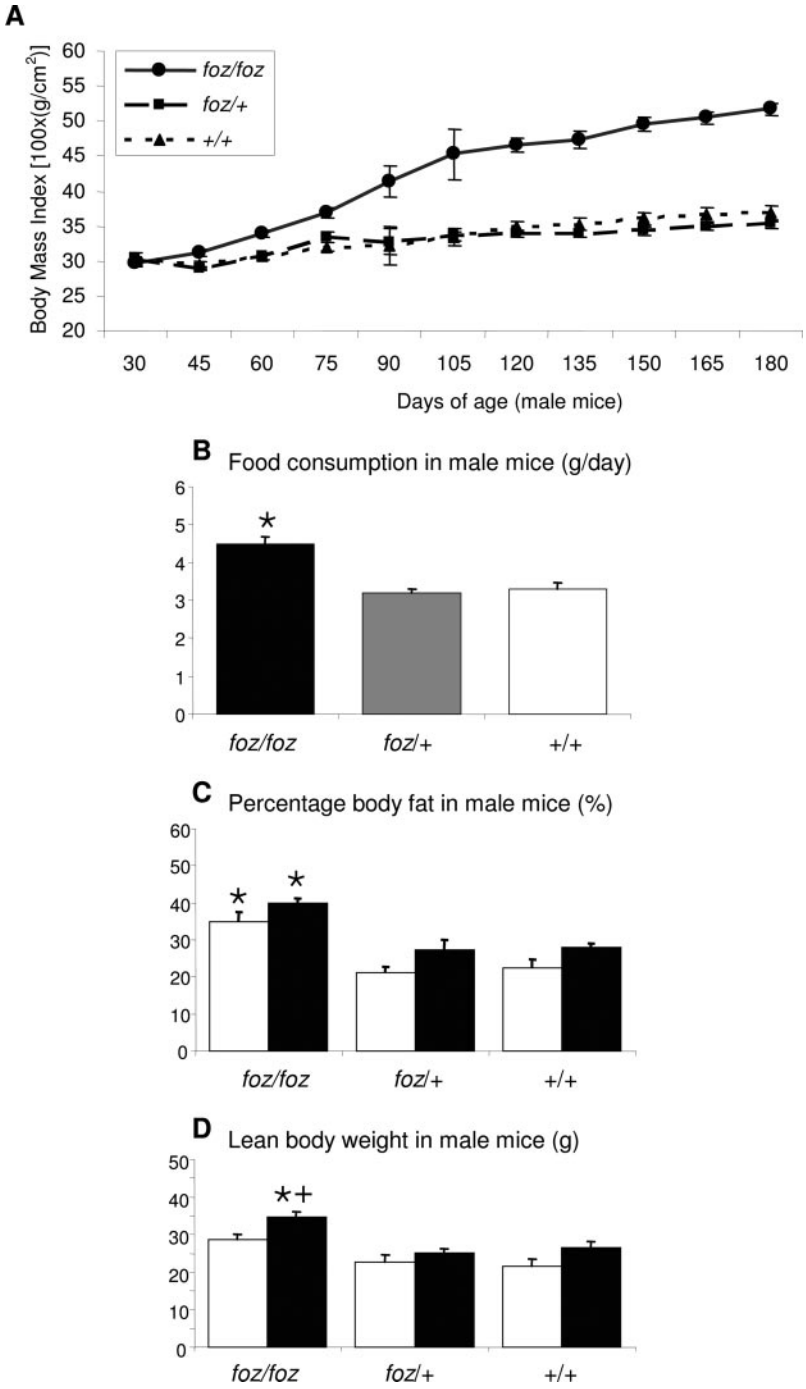

Fig. 3. Effect of Genotype on BMI, Food Consumption, and Body Composition in Male Mice

A, BMI growth curves for male mice of each genotype (n = 10–12 per group). B, Increased food consumption in male mice (age 180 d, n = 6 per group; individually housed mice, mean values from food consumption in 3 consecutive days). *Alms1 foz/foz* mice consumed significantly more food than *foz*/+ and +/+ control mice (*, $P < 0.001$). C, Percentage of body fat measured by DXA scanning. Both young (70 d old, *white bars*) and old (250 d old, *black bars*) *Alms1 foz/foz* mice have significantly higher percentage of body fat compared with *foz*/+ and +/+ controls (*, $P < 0.01$). D, Lean body weight analysis shows no significant difference between the three genotypes at younger age (70 d, *white bars*). Only older (250 d old, *black bars*) male *Alms1 foz/foz* mice have significantly higher lean body weight compared with *foz*/+ (*, $P < 0.01$) and +/+ (+, $P < 0.05$) control mice.

Fat aussie mice exhibited significant hyperinsulinemia before the onset of hyperglycemia. Male *Amls1 foz/foz* mice became significantly hyperinsulinemic compared with +/+ littermates as early as 60 d of age (data not shown). At a later age, hyperinsulinemia becomes more severe (age 90 d: 3612 ± 607 pmol/liter

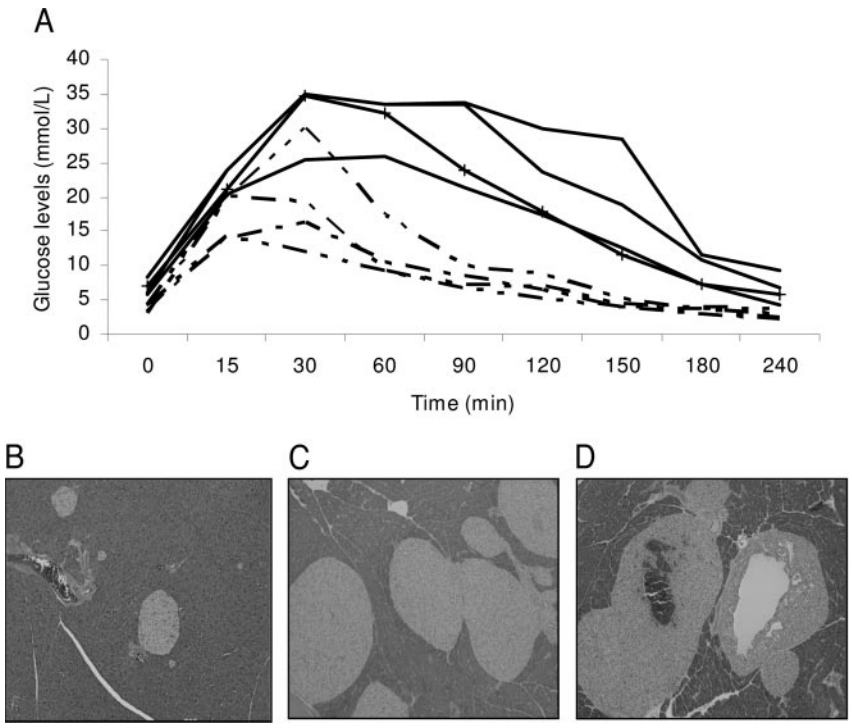

Fig. 4. Glucose Metabolism Disturbances in *Alms1 foz/foz* Mice

A, Impaired glucose tolerance in prediabetic *Alms1 foz/foz* mice (*solid lines*) compared with wild-type controls (*dotted lines*). B–D, Hematoxylin and eosin-stained sections of representative pancreatic islets from +/+ (B) and *Alms1 foz/foz* (C and D) mice showing extreme islet hyperplasia (C) and cystic changes (D).

vs. 457 ± 84 pmol/liter; n =10 mice per group; $P <$ 0.001). In female *Alms1 foz/foz* mice, hyperinsulinemia became significant at age 90 d (3644 ± 373 pmol/liter *vs.* 499 ± 162 pmol/liter; n =10 mice per group; $P <$ 0.001). Histological analyses revealed that the pancreatic islets were enormously hypertrophied in diabetic *Alms1 foz/foz* mice (Fig. 4, B–D), indicating a compensatory β-cell growth response. Many islets formed central cystic spaces. Collectively, these data indicate a compensatory hyperinsulinemia for insulin resistance in the mutant mice, which failed to maintain normal glycemia in older mice.

In addition to obesity and diabetes, *Alms1 foz/foz* mice developed other metabolic abnormalities. On a normal diet, female and male mutant mice had 50% higher cholesterol levels compared with heterozygotes and wild-type littermates (Fig. 5, A and B). This was accentuated by high-fat feeding: cholesterol levels in mutant mice fed with a high-fat diet were up to 200% higher than cholesterol levels in controls ($P < 0.01$; Fig. 5, C and D). Serum triglyceride concentrations remained normal in mutant mice, even when fed a high-fat diet (data not shown). Both male and female mutant mice had enlarged, pale livers, and histologic examination revealed moderate to severe steatosis (data not shown).

Male Infertility in *Fat Aussie* Alms1 Mutant Mice Is Attributable to a Primary Defect in Spermatogenesis

All attempts to breed *Alms1 foz/foz* males (25 mice, age 60–180 d) were unsuccessful whereas heterozygote males produced normal sized litters (data not shown). Testes from male *Alms1 foz/foz* mice were nearly one third the size and weight of those from heterozygotes or wild-type mice (Fig. 6, A and B). Histological analysis identified that there was an overall decrease in germ cells at all stages of spermatogenesis beyond the spermatogonial stage. Of those germ cells that progressed through meiosis, the vast majority disappeared at step 8–9 of spermiogenesis, namely in the conversion of the round to elongating spermatids (Fig. 6, C and D). The occasional almost mature spermatid was seen in the epithelium, but these must have been reabsorbed as spermatozoa were not found in the epididymis (data not shown). The germ cell loss was consistent with the increase in TUNEL-positive cells indicative of apoptosis (Fig. 6, E and F).

Electron microscopy confirmed the presence of significant numbers of degenerating germ cells at the primary spermatocyte and spermatid stages (Fig. 7, A and B). Significant numbers of spermatids showed two nuclei with acrosomal caps surrounded by a continu-

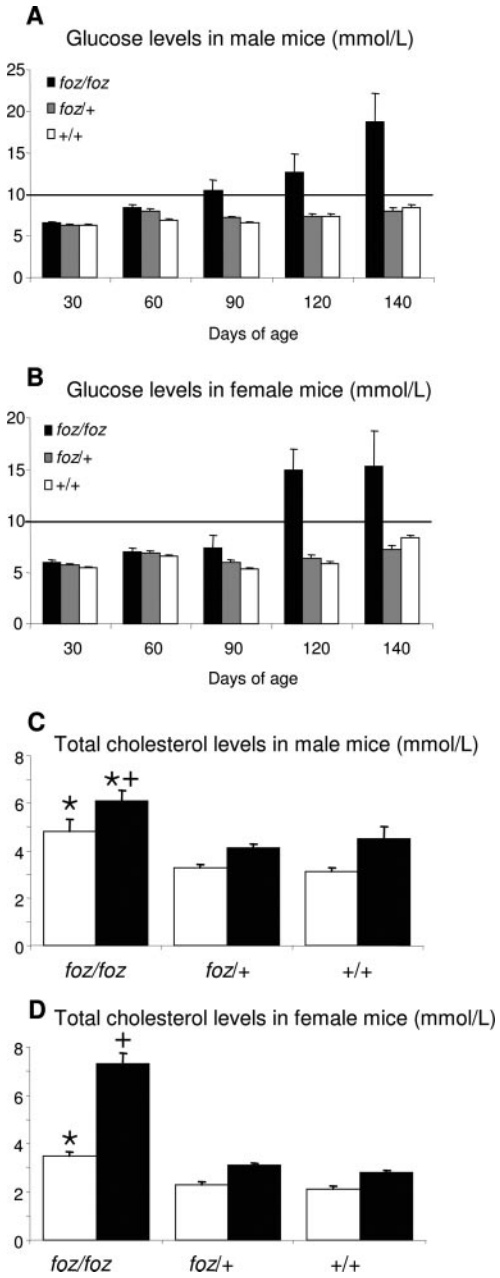

Fig. 5. Metabolic Disturbances in *Alms1 foz/foz* Mice

A and B, Glucose levels in male (A) and female mice (B) of the indicated genotype. *Horizontal black line* indicates the borderline glucose levels (10 mmol/liter) above which mice were considered diabetic (n = 10 mice per group). C, Serum total cholesterol levels in male mice of the indicated genotypes (n = 10 mice per group, age 130 d). Male *Alms1 foz/foz* mice fed normal diet (*white bars*) have significant hypercholesterolemia compared only to +/+ controls (*, $P < 0.05$). When fed high-fat diet (*black bars*) *Alms1 foz/foz* mice have significantly increased total cholesterol levels compared with both *foz*/+ (*, $P < 0.001$) and +/+ (+, $P < 0.05$) control mice. D, Serum total cholesterol levels in female mice (n = 10 mice per group, age 130 d). Female *Alms1 foz/foz* mice fed normal diet (*white bars*) have significant hypercholesterolemia compared with both *foz*/+ and +/+ control mice (*, $P < 0.01$). The most severe hypercholesterolemia is found in female *Alms1 foz/foz* mice fed high-fat diet (*black bars*; +, $P < 0.001$).

ous plasma membrane (Fig. 7C), suggesting a failure of cytokinesis. The tails of the few elongated spermatids that were observed showed abnormal increases in the number of outer dense fibers (>9) in the midpiece of spermatids, and their shape and size varied considerably in contrast to spermatids from a comparable stage in wild-type mice (Fig. 7, D and E). The microtubule arrangements in the axoneme were usually normal, but occasionally, variations in the numbers or placement of doublet microtubules were found (Fig. 7, D and E). The mitochondria of spermatids showed bizarre profiles with a marked increase in the electron density and sparse inner mitochondrial membranes (Fig. 7, E and F). It was not possible to determine whether the mitochondrial phenotype was due to a developmental defect or as a consequence of degeneration.

The electron microscopic features of the Sertoli cells were not appreciably different from those of wild-type mice; however, there was a marked increase in the Sertoli cell content of acetylated tubulin, as demonstrated by immunohistochemistry (Fig. 6H). This was in striking contrast to well-defined localization of acetylated tubulin to elongated spermatid tails of wild-type testes (Fig. 6G). Cells within the testicular interstitium appeared normal, an observation that was consistent with normal serum testosterone levels. These observations, in combination with normal FSH and inhibin levels (data not shown) in foz/foz mice, strongly suggested that male infertility was not secondary to a failure of the hypothalamo-pituitary-gonadal axis, but due to a primary testicular defect. The possibility remains, however, that spermatogenesis was further compromised in older mice after the development of diabetes and a decline in general health.

Young female *Alms1 foz/foz* mice were fertile, although litter sizes were smaller than those of corresponding heterozygotes and wild type mice. After development of obesity, female mutant mice were infertile. At this stage, their ovaries contained primary and secondary follicles but were devoid of corpora lutea, indicating an anovulatory state (data not shown).

Audiological Findings

Because deafness is often a presenting sign in human Alström syndrome, and hearing function in the inner ear depends on functional hair cell cilia, we conducted an auditory-evoked brainstem response potential analysis in *fat aussie* mice. At the age of 150 d *Alms1 foz/foz* and +/+ mice had comparable hearing thresholds [26 ± 1.5 decibels (dB) *vs.* 27.5 ± 4.0 dB; $P > 0.05$]; however, older *Alms1 foz/foz* mice (360 d of age) had significantly increased hearing threshold (67.1 ± 6.1 dB *vs.* 40.8 ± 6.0 dB; n = 6–7 mice per group; $P < 0.05$). All of the *Alms1 foz/foz* mice (n = 7) had a hearing threshold of at least 50 dB, three mice had a threshold of at least 80 dB. The findings of reduced hearing in older mutant mice are

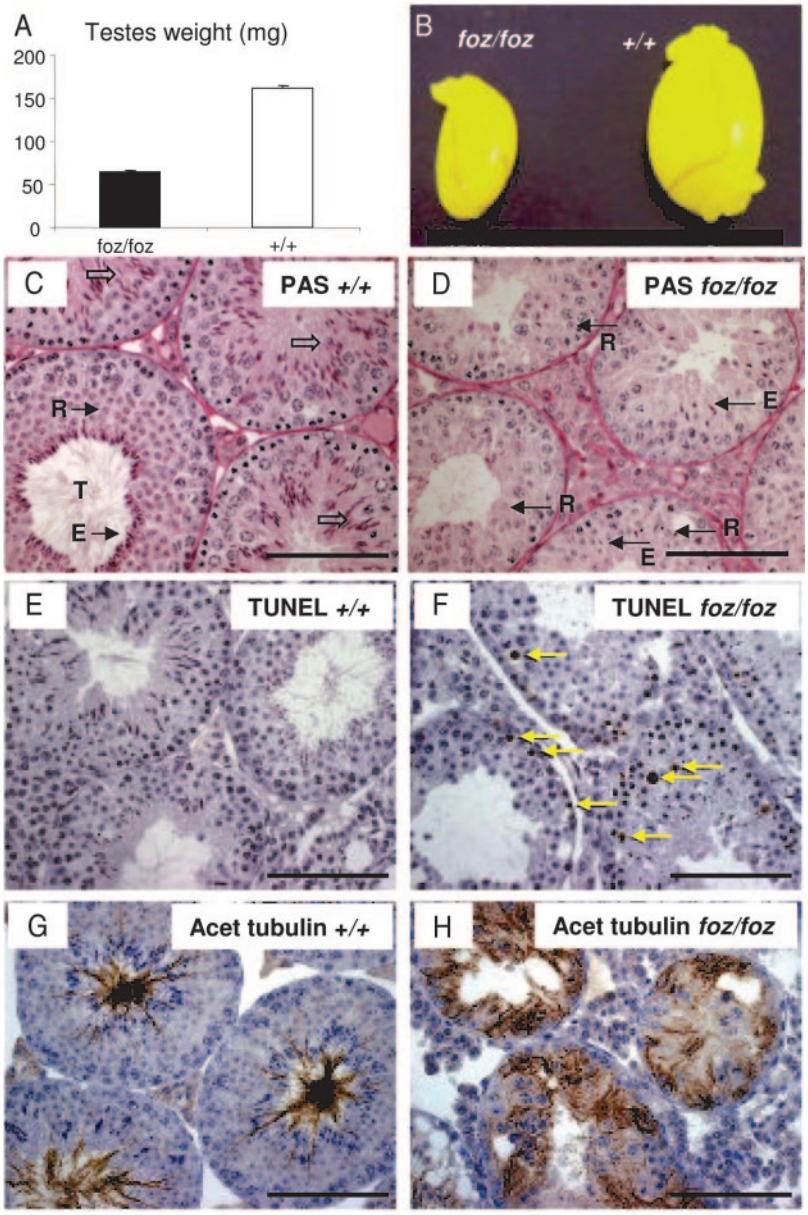

Fig. 6. *Alms1* Mutations Result in Male Infertility as a Result of Spermatogenic Failure

A, Testis weight from *Alms1 foz/foz* and wild-type mice. B, Hypogonadism in *Alms1 foz/foz* mice. C, PAS-stained testis from a wild-type mouse showing full spermatogenesis. D, Spermatogenesis in *Alms1 foz/foz* mice showing loss of germ cells at all stages of spermatogenesis, followed by a more significant germ cell arrest corresponding to the transition of round spermatids to elongated spermatids. E, TUNEL-stained wild-type testis showing a relative lack of apoptotic cells. F, *Alms1 foz/foz* mice showed a relative increase in apoptotic cells (*arrows*). G, Immunostaining for acetylated tubulin in wild-type testis showing localization to the tails of elongated spermatids. H, Immunostaining for acetylated tubulin in *foz/foz* testes showing aberrant expression within the cytoplasm of Sertoli cells. R, Round spermatids; *open arrows*, elongating spermatids; E, elongated spermatids; T, T-sperm tails; *arrows*, TUNEL-positive, apoptotic germ cells. *Scale bar*, 100 mm. Acet, Acetylated; PAS, periodic acid Schiff.

consistent with those reported in the *Alms1* gene-trapped model (19).

DISCUSSION

Characterization of *fat aussie*, a new murine model of Alström syndrome caused by a spontaneous mutation of the *Alms1* gene similar to the mutations seen in human patients, provides novel insights into the etiopathogenesis of several key features of Alström syndrome, including obesity, insulin resistance with disordered glucose metabolism, and cholesterol disturbances. Furthermore, it provides a mechanism to explain infertility in males with Alström syndrome, namely spermatogenic failure, which in humans would manifest as azoospermia. Metabolic

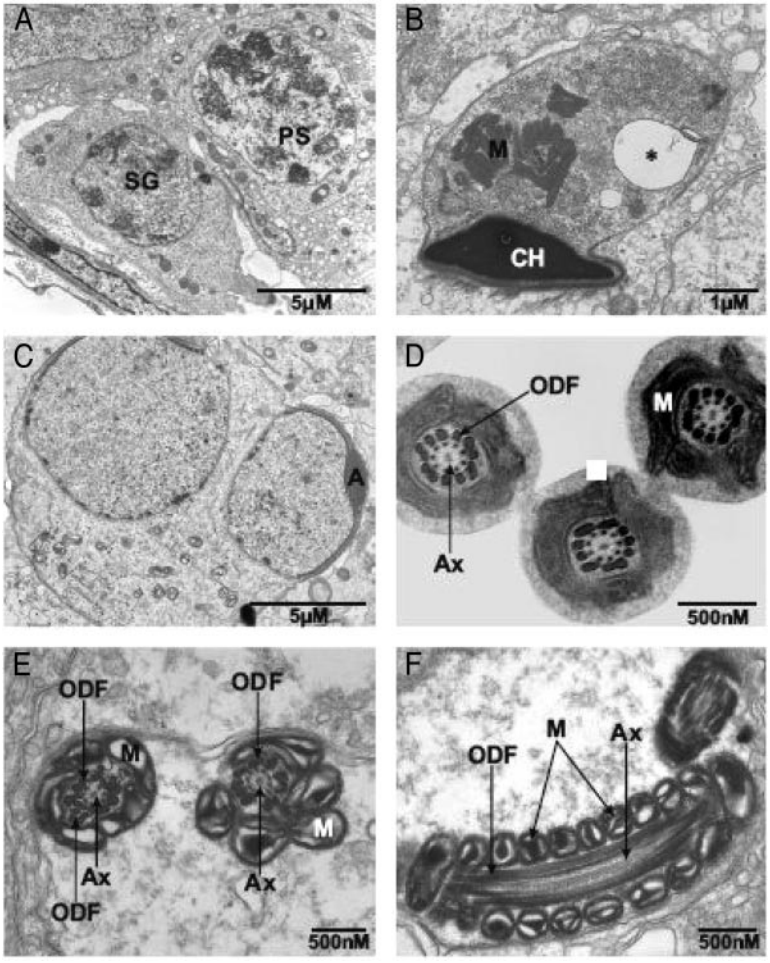

Fig. 7. Ultrastructural Abnormalities in *Alms1 foz/foz* Mouse Testes

A, Germ cell degeneration was visible in all cells beyond the spermatogonia stage of spermatogenesis as indicated by the presence of apoptotic primary spermatocytes. B, Presence of degenerating elongated spermatids. C, A failure of cytokinesis was frequently observed in round spermatids. D, Cross-sectional profiles of elongated spermatids in the normal testis showing the presence of a normal 9+2 axonemal structure surrounded by nine evenly spaced outer dense fibers and helically arranged mitochondria. E, Within the few elongated spermatids that formed in *Alms1 foz/foz* mice, the vast majority contained abnormal cross-sectional profiles typified by the abnormal numbers and placement of outer dense fibers and abnormal/degenerating mitochondria. Most axonemal profiles were relatively normal, however, the occasional misplaced microtubule doublet was observed. F, A longtitudinal profile of a *foz/foz* elongated spermatid tail showing a relatively normal axonemal microtubule arrangement. A, acrosome; Ax, axoneme; CH, condensed sperm head; M, mitochondria; ODF, outer dense fiber; PS, primary spermatocyte; SG, spermatogonia.

studies into the basis of obesity in Alström syndrome have been inconclusive. Although some have proposed hyperphagia as a possible mechanism underlying the early childhood obesity, the evidence for this remains anecdotal (1, 2, 11). We show that the *Alms1* mutation causes hyperphagia that precedes obesity, which could explain the weight gain and morbid obesity due to increased adiposity, with a minor contribution from increased lean mass only in older mice. Although further food consumption analysis is necessary to establish the cause and effect relationship between the hyperphagia and the obesity, our findings suggest that ALMS1 may play a role in the control of food intake and that hyperphagia could be a cause for the early-onset obesity, consistent with the findings in mouse models of the related Bardet-Biedl syndrome (20–22). Hyperphagia has been difficult to verify in the few human Alström syndrome patients that have been described clinically so far.

Like human Alström syndrome, *Alms1 foz/foz* mice developed insulin resistance and compensatory hyperinsulinemia. With increasing age both male and female mice developed type 2 diabetes. This spontaneous mutant model of Alström syndrome is similar to the human syndrome with respect to the development of diabetes (1) and differs from *Alms1* gene-trapped mice (19) in which only male mice develop diabetes. The phenotypic difference in the mouse models may relate to either mouse interstrain differences or to the hypomorphic nature of the *Alms1* gene-trapped allele (19).

In the present model we observed a massive expansion of pancreatic islets and interestingly a formation of unusual cystic cavities in *Alms1 foz/foz* mice. The relevance of these cystic cavities is unknown but may be a specific primary feature of loss of *Alms1* function in islets of Langerhans. Hypercholesterolemia, but not hypertriglyceridemia, is a conspicuous metabolic abnormality in *Alms1 foz/foz* mice, although the reasons for this are unclear. The possibility arises that *Alms1* may play additional roles in cellular lipid partitioning (*e.g*. fatty acid transport and lipoprotein assembly and secretion), but this requires further investigation. In support of this hypothesis, we have recently noted that high-fat intake exacerbates hepatic steatosis in the *Alms1 foz/foz* mouse (23); this may provide insight into the pathogenesis of nonalcoholic fatty liver disorders, and more detailed studies of hepatic lipid partitioning in this model are underway.

The infertile state of female mice may be linked to obesity and the related changes in insulin resistance, because obese women with polycystic ovarian disease show infertility (24). Further studies are required to explore this potential link.

Our data demonstrate that the infertility in male *Alms1 foz/foz* mice was due to a spermatogenic disruption. This view is supported by the normal levels of FSH, immunoreactive inhibin, and testosterone. Although there was a generalized loss of germ cells, there was a more severe decrease in the conversion of round to elongated spermatids. However, it is important to note that spermatids can, on rare occasions, generate a tail structure virtually completing spermatogenesis, indicating that the distal centriole of the spermatid can generate an axoneme. This is consistent with an earlier report that *Alms1* gene-trapped mice assemble cilia normally (19) and our observations of apparently normal auditory function at a young age.

The failure of the majority of germ cells to complete the conversion of a round to an elongating spermatid is of interest. It is at this stage that the manchette forms around the nucleus of the spermatid and the sperm tail/axoneme nucleates (25). The manchette is a microtubular structure that is hypothesized to be involved in nuclear elongation and in the transport of proteins involved in outer dense fiber formation in the tail (25). Similarly, the assembly of the sperm tail in general requires transport of proteins from the cytoplasm of spermatids down the cytoplasmic canal or sheath surrounding the axoneme of the sperm tail in what is presumably a microtubule-dependent process. The specific stage of this arrest coupled with the observation of numerous examples of a failure of cytokinesis at meiosis, abnormal outer dense fiber shape and number in elongated spermatids, and the presence of aberrantly expressed acetylated tubulin in Sertoli cells is strongly suggestive of abnormal microtubular dynamics. For the later observation, however, it cannot be ruled out that the presence of acetylated tubulin within Sertoli cells is a consequence of germ cell phagocytosis.

ALMS1 is a component of centrosomes and the basal bodies of cilia (17–19). A single nonmotile primary cilium is present on most cells in the body, where localization of specific receptors suggests it serves as a sensory device or antenna (26–29). Primary cilia are found on fat-storing hepatocytes (30–33), pancreatic β-cells (34, 35), and are prominent on leptin-responsive hypothalamic neurons that control satiety (36–41). The primary neuronal cilium is considered to be a relict of ancestral neurons—a nonfunctional remnant of the Cnidarian nerve net (the skin brain). The cilia from these cells have a distinct function in sensing pheromones, food, and fluid flow. Primary neuronal cilia represent an active region of the neuron containing ATP-requiring mechanisms to transport molecules, including potential signals, inside the cell (40). Some receptors, such as somatostatin 3 receptors and 5-hydroxytryptamine 6 receptors, are selectively concentrated on these surface structures (41). It is therefore tempting to hypothesize that primary neuronal cilia have a role in sensing or tuning peripheral satiety signals. Similarly, dysfunction of the primary cilia on pancreatic endocrine cells and their ductal cell precursors may cause hyperproliferation (34, 35), leading to the large, cystic islets and hyperinsulinemia in *fat aussie*. The tail of sperm cells is a motile flagellum related to motile primary cilia, providing a more readily understood link between the *Alms1* mutation and defects in development of motile spermatozoa.

In summary, we have identified mice with a spontaneous mutation in the *Alms1* gene. *Alms1 foz/foz* mice of both genders exhibit hyperphagia associated with profound obesity, insulin resistance, diabetes with morphologic changes in pancreatic islets, and several features of metabolic syndrome. Male *fat aussie* mice are sterile due to primary spermatogenic abnormalities. The present observations in a spontaneous mouse model of Alström syndrome therefore provide insight into some of the biological functions of ALMS1 and how these could be related to the pathogenesis of human obesity, diabetes, and infertility.

MATERIALS AND METHODS

Animals

The *fat aussie* mouse strain was maintained in the Animal Facility at The Canberra Hospital under specific pathogen-free conditions in a 12-h light/12-h dark cycle. Mice were fed normal chow (5.4% fat; energy content 12 megajoule/kg) or high-fat diet (21% fat; energy content 19.4 megajoule/kg) and had access to water *ad libitum*. All animal procedures were approved by the Animal Ethics and Experimentation Committee of the Australian National University and conformed to the highest international standards of humane care.

Mapping and Sequencing

Chromosomal linkage of the *foz* mutation was established in an F_2 intercross between NOD and C57Bl/10 mice using a

panel of 88 polymorphic short tandem repeat markers spaced at 20–30 centimorgans throughout the mouse genome. Fine mapping was done using F_3 recombinants and additional polymorphic markers spaced at 1 centimorgan within the candidate interval (D6Mit17, D6Mit209, D6Mit281, D6Mit29, D6Mit213, and D6Mit102). Total RNA from *foz/foz* and NOD liver was prepared using TRIzol (Invitrogen Life Technologies, Carlsbad, CA) and reverse transcribed using random hexamers. Alms1 cDNA was PCR amplified and sequenced with primers designed to be complementary to the NCBI Alms1 transcript.

Screening Mice for the *foz* Mutation

A mutation-specific PCR using primers flanking the deletion (forward, ACA ACT TTT CAT GGC TCC AGT; reverse, TTG GCT CAG AGA CAG TTG AAA) was designed to screen mice for the presence of *foz* mutation (Fig. 1D). The PCR conditions were 95 C for 5 min, followed by 35 cycles of 95 C, 55 C, and 72 C for 1 min each and 72 C for 10 min. PCR products were visualized on 4% agarose gel.

Food Consumption

Food consumption studies were carried out in individually housed mice. Measurements were performed on 3 consecutive days. Each of the analyzed groups (both sexes and three genotypes) included six mice at 180 d of age.

BMI Analysis

Weight and nasal-anal length data were monitored from 30–180 d of age. Nasal-anal length was measured to the nearest millimeter in anesthetized mice. BMI values were calculated according to the formula 100*weight (in grams)/length (in cm^2) and expressed in 100 g/cm^2 units. Each of the analyzed groups (both sexes and three genotypes) included 10–12 mice.

Glucose Tolerance Test

ip Glucose tolerance test (2 mg glucose/g body weight) was carried out in mice fasted for 18 h. Glucose levels were determined at time points 0, 15, 30, 90, 120, and 180 min using an Advantage II glucometer (Roche, Indianapolis, IN).

DXA Scanning

DXA scans were performed in young (70–90 d old) and old (250 d old) male and female mice fed on chow (five mice in each genotype group) as described previously (42). Mice were killed immediately before placing them in the animal holder in the DXA scanner (PIXImus mouse densitometer, GE Medical Systems Lunar, Madison, WI).

Laboratory Analyses

Overnight fasted blood samples were obtained by retroorbital bleeding at different time points. Serum lipid profiles were determined using standard clinical chemistry procedures (Department of Clinical Chemistry, The Canberra Hospital). Random blood glucose levels were monitored at regular 15-d intervals using an Advantage II glucometer (Roche, Indianapolis, IN). Insulin levels were measured by commercial ELISA (Mercodia, Uppsala, Sweden), serum total testosterone concentrations were measured with a mouse-specific kit (ICN Biomedicals, Costa Mesa, CA), and serum FSH and inhibin levels were determined as described previously (43, 44).

Histological Analysis

Testes were fixed in Bouin's fixative overnight and processed into paraffin using standard methods. Sections (5 μm) were stained with periodic acid Schiff's reagent and counterstained with hematoxylin. Other organs were fixed in 10% neutral-buffered formalin and stained with hematoxylin and eosin using standard methods.

Testis Immunohistochemistry

Testis sections were stained for acetylated tubulin using monoclonal mouse antiacetylated tubulin Ig (clone 6–11B; Sigma Chemical Co., St. Louis, MO) at a dilution of 1:5000 and the DAKO EnVision kit as recommended by the manufacturer (DAKO Corp., Carpinteria, CA). Sections were counterstained with hematoxylin. Cells undergoing apoptosis were visualized using the Apotag kit TUNEL assay as recommended by the manufacturer (Intergen Co., Purchase, NY).

Testis Electron Microscopy

Testes from wild-type and *foz/foz* animals were fixed and processed for electron microscopy as described previously (45) with the exception that testes were decapsulated before fixation.

Auditory Brain Stem Response

Click-evoked auditory brainstem response thresholds were determined using a Navigator Pro diagnostic system (Biologic Systems Corp., Mundelain, IL) as described previously (46).

Statistical Analyses

Results are presented as mean $\pm$ SEM. Comparisons between the groups using parametric (Bonferroni's multiple comparison test) or nonparametric (Dunn's multiple comparison test) one-way ANOVA (PRISM version 4.0; GraphPad Software, Inc., San Diego, CA). When standard skewness and kurtosis values were within the -2 to $+2$ range, distributions were considered normal. P values < 0.05 were considered statistically significant.

Acknowledgments

We thank David Buckle and Belinda Whittle from the Australian Phenomics Facility for technical advice with gene mapping; Associate Professor Herbert Herzog from the Garvan Institute and Professors Geoff Farrell and Christopher Nolan from the Australian National University Medical School for scientific discussions; Jo Merriner from the Monash Institute of Medical Research for electron microscopy and immunohistochemistry assistance; and Kimberly Hewitt for assistance in maintaining the mouse colony.

Received December 7, 2005. Accepted February 22, 2006.

Address all correspondence and requests for reprints to: Dr. Todor Arsov, Immunogenomics Laboratory, John Curtin School of Medical Research, Australian National University, Mills Road, P.O. Box 334, Canberra ACT 2601, Australia. E-mail: todor.arsov@anu.edu.au.

This work was supported by grants from the National Health and Medical Research Council (to C.C.G.), the Juvenile Diabetes Research Foundation (to C.C.G.), and the Canberra Hospital Private Practice Fund (to N.P.).

Conflict of Interest Statement: The findings presented in the paper are original and have not been previously submitted for publication; all authors concur with the submission, and none have any conflict of interest with publication of these findings.

REFERENCES

1. Marshall JD, Bronson RT, Collin GB, Nordstrom AD, Maffei P, Paisey RB, Carey C, Macdermott S, Russell-Eggitt I, Shea SE, Davis J, Beck S, Shatirishvili G, Mihai CM, Hoeltzenbein M, Pozzan GB, Hopkinson I, Sicolo N, Naggert JK, Nishina PM 2005 New Alstrom syndrome phenotypes based on the evaluation of 182 cases. Arch Intern Med 163:675–683
2. Marshall JD, Ludman MD, Shea SE, Salisbury SR, Willi SM, LaRoche RG, Nishina PM 1997 Genealogy, natural history and phenotype of Alström syndrome in a large Acadian kindred and three additional families. Am J Med Genet 73:150–161
3. Paisey RB, Carey CM, Bower L, Marshall J, Taylor P, Maffei P, Mansell P 2004 Hypertriglyceridemia in Alström syndrome: causes and associations in 37 cases. Clin Endocrinol (Oxf) 60:228–231
4. Russell-Eggitt IM, Clayton PT, Coffey R, Kriss A, Taylor DS, Taylor JF 1998 Alström syndrome. Report of 22 cases and literature review. Ophthalmology 105: 1274–1280
5. Benso C, Hadjadj E, Conrath J, Denis D 2002 Three new cases of Alström syndrome. Graefes Arch Clin Exp Ophthalmol 240:622–627
6. Satman I, Yilmaz MT, Gursoy N, Karsidag K, Dinccag N, Ovali T, Karadeniz S, Uysal V, Bugra Z, Okten A, Devrim, S 2002 Evaluation of insulin resistant diabetes mellitus in Alström syndrome: a long term prospective follow-up of three siblings. Diabetes Res Clin Pract 56:189–196
7. Tai TS, Lin SY, Sheu WHH 2003 Metabolic effects of growth hormone therapy in an Alström syndrome patient. Horm Res 60:297–301
8. Bond J, Flintoff K, Higgins J, Scott S, Bennet C, Parsons J, Mannon J, Jafri H, Rashid Y, Barrow M, Trembath R, Woodruff G, Rossa E, Lynch S, Sheilds J, Newbury-Ecob R, Falconer A, Holland P, Cockburn D, Karbani G, Malik S, Ahmed M, Roberts E, Taylor G, Woods CG 2005 The importance of seeking ALMS1 mutations in infants with dilated cardiomyopathy. J Med Genet 42:e10
9. Hoffman JD, Jacobson Z, Marshall JD, Kaplan P 2005 Familial variable expression of dilated cardiomyopathy in Alström syndrome: a report of four sibs. Am J Med Genet 135:96–98
10. Quiros-Tejeira RE, Vargas J, Ament ME 2001 Early-onset liver disease complicated with acute liver failure in Alström syndrome. Am J Med Genet 101:9–11
11. Collin GB, Marshall JD, Cardon LR, Nishina PM 1997 Homozygosity mapping of Alström syndrome to chromosome 2p. Hum Mol Genet 6:213–219
12. Collin GB, Marshall GD, Nishina PM, Naggert JK 1998 Human DCTN1: genomic structure and evaluation as a candidate for Alström syndrome. Genomics 53:359–364
13. Collin GB, Marshall GD, Naggert JK, Nishina PM 1999 TGFA: exon-intron structure and evaluation as a candidate gene for Alström syndrome. Clin Genet 55:61–62
14. Collin GB, Marshall JD, Boerkoel CF, Levin AV, Weksberg R, Greenberg J, Michaud JL, Naggert JK, Nishina PM 1999 Alström syndrome: further evidence for linkage to human chromosome 2p13. Hum Genet 105:474–479
15. Collin GB, Marshall JD, Ikeda A, So WV, Russell-Eggitt I, Maffei P, Beck S, Boerkoel CF, Sicolo N, Martin M, Nishina PM, Naggert JK 2002 Mutations in ALMS1 cause obesity, type 2 diabetes and neurosensory degeneration in Alström syndrome. Nat Genet 31:74–78
16. Hearn T, Renforth GL, Spalluto C, Hanley NA, Piper K, Brickwood S, White C, Connolly V, Taylor JF, Russell-Eggitt I, Bonneau D, Walker M, Wilson DI 2002 Mutation of ALMS1, a large gene with a tandem repeat encoding 47 amino acids, causes Alström syndrome. Nat Genet 31:79–83
17. Andersen JS, Wilkinson CJ, Mayor T, Mortensen P, Nigg EA, Mann M 2003 Proteomic characterization of the human centrosome by protein correlation profiling. Nature 426:570–574
18. Hearn T, Spalluto C, Phillips VJ, Renforth GL, Copin N, Hanley NA, Wilson DI 2005 Subcellular localization of ALMS1 supports involvement of centrosome and basal body dysfunction in the pathogenesis of obesity, insulin resistance and type 2 diabetes. Diabetes 54:1581–1587
19. Collin GB, Cyr E, Bronson R, Marshall JD, Gifford EJ, Hicks W, Murray SA, Zheng QY, Smith RS, Nishina PM, Naggert JK 2005 Alms1 disrupted mice recapitulate human Alström syndrome. Hum Mol Genet 14:2323–2333
20. Nishimura YD, Fath M, Mullins FR, Searby C, Andrews M, Davis R, Andorf LJ, Mykytyn K, Swiderski R, Yang B, Carmi R, Stone ME, Sheffield CV 2004 Bbs2-null mice have neurosensory deficits, a defect in social dominance, and retinopathy associated with mislocalisation of rhodopsin. Proc Natl Acad Sci USA 101:16588–16593
21. Mykytyn K, Mullins FR, Andrews M, Chiang PA, Swiderski ER, Yang B, Braun T, Casavant T, Stone ME, Sheffield CV 2004 Bardet-Biedl syndrome type 4 (BBS4)-null mice implicate Bbs4 in flagella formation but not global cilia assembly. Proc Natl Acad Sci USA 101:8664–8669
22. Fath AM, Mullins FR, Searby C, Nishimura YD, Wei J, Rahmouni K, Davis ER, Tayeh KM, Andrews M, Yang B, Sigmund DC, Stone ME, Sheffield CV 2005 Mkks-null mice have a phenotype resembling Bardet-Biedl syndrome. Hum Mol Genet 14:1109–1118
23. Arsov T, Larter ZC, Nolan JC, Petrovsky N, Goodnow CC, Teoh CN, Yeh MM, Farrell CG 2006 Adaptive failure to high fat diet characterizes steatohepatitis in Alms1 mutant mice. Biochem Biophys Res Commun 342: 1152–1159
24. Adams J, Polson DW, Franks S 1986 Prevalence of polycystic ovaries in women with anovulation and idiopathic hirsutism. Br Med J (Clin Res Ed) 293:355–359
25. de Kretser DM, Loveland K, O'Bryan MK, Kerr J 2006 The cytology of the testis and intrinsic control mechanisms. In: Neill DJ, Challis RGJ, de Kretser DM, Pfaff WD, Richards SJ, Plant MT, Wassarman MP, eds. The physiology of reproduction. 3rd ed. San Diego: Elsevier
26. Pan J, Wang Q, Snell WJ 2005 Cilium-generated signalling and cilia related disorders. Lab Invest 85:452–463
27. Salisbury JL 2004 Primary cilia: putting sensors together. Curr Biol 14:R765–R767
28. Pazour GJ, Witman GB 2003 The vertebrate cilium is a sensory organelle. Curr Opin Cell Biol 15:105–110
29. Fuchs JL, Schwark HD 2004 Neuronal primary cilia: a review. Cell Biol Int 28:111–118
30. de Brito Gitirana L 1987 The first report of the occurrence of cilium in fat-storing cells in the reptilian liver (*Eumeces algeriensis*, Daudin 1802). Arch Histol Jpn 50:359–361
31. Tobe K, Tsuchiya T, Itoshima T, Nagashima H, Kobayashi T 1985 Electron microscopy of fat-storing cells in liver diseases with special reference to cilia and cytoplasmic cholesterol crystals. Arch Histol Jpn 48:435–441
32. Tanuma Y, Ohata M, Ito T 1981 An electron microscopic study of the kitten liver with special reference to fat-storing cells. Arch Histol Jpn 44:23–49
33. Geerts A, Bouwens L, Wisse E 1990 Ultrastructure and function of hepatic fat-storing and pit cells. J Electron Microsc Tech 14:247–256
34. Cano DA, Murcia NS, Pazour GJ, Hebrok M 2004 Orpk mouse model of polycystic kidney disease reveals essential role of primary cilia in pancreatic tissue organization. Development 131:3457–3467

35. Zhang Q, Davenport JR, Croyle MJ, Haycraft CJ, Yoder BK 2005 Disruption of IFT results in both exocrine and endocrine abnormalities in the pancreas of Tg737(orpk) mutant mice. Lab Invest 85:45–64
36. Stepanyan Z, Kocharyan A, Pyrski M, Hubschle T, Watson AM, Schulz S, Meyerhof W 2003 Leptin-target neurons of the rat hypothalamus express somatostatin receptors. J Neuroendocrinol 15:822–830
37. Amat P, Blazquez JL, Pelaez B, Sanchez A, Amat-Peral H, Amat-Peral P, Pastor FE 1998 Ultrastructural features of rat arcuate nucleus during pregnancy. Ital J Anat Embryol 103:311–324
38. Suarez I, Fernandez B, Perez-Batista MA, Azcoitia I 1985 Ciliated neurons in the paraventricular nuclei in old hamsters. J Submicrosc Cytol 17:351–356
39. Lafarga M, Hervas JP, Crespo D, Villegas J 1980 Ciliated neurons in supraoptic nucleus of rat hypothalamus during neonatal period. Anat Embryol (Berl) 160:29–38
40. Whitfield JF 2004 The neuronal primary cilium—an extrasynaptic signalling device. Cell Signal 16:763–767
41. Brailov I, Bancila M, Brisorgueil MJ, Miquel MC, Hamon M, Verge D 2000 Localization of 5-HT6 receptors at the plasma membrane of neuronal cilia in the rat brain. Brain Res 872:271–275
42. Nagy TR, Clair AL 2000 Precision and accuracy of dual-energy X-ray absorptiometry for determining in vivo body composition of mice. Obes Res 8:392–398
43. Robertson KM, O'Donnell L, Simpson ER, Jones ME 2002 The phenotype of the aromatase knockout mouse reveals dietary phytoestrogens impact significantly on testis function. Endocrinology 143:2913–2921
44. Robertson DM, Hayward S, Irby D, Jacobsen J, Clarke L, McLachlan RI, de Kretser DM 1988 Radioimmunoassay of rat serum inhibin: changes after PMSG stimulation and gonadectomy. Mol Cell Endocrinol 58:1–8
45. O'Bryan MK, Sebire KL, Meinhardt A, Edgar KA, Keah HH, Hearn MTV, de Kretser DM 2001 Tpx-1 is a component of the outer dense fibers and acrosome of rat spermatozoa. Mol Reprod Dev 58:116–125
46. Hildebrand MS, de Silva MG, Klockars T, Rose E, Price M, Smith RJ, McGuirt WT, Christopoulos H, Petit C, Dahl HH 2004 Characterisation of DRASIC in the mouse inner ear. Hear Res 190:149–160

Molecular Endocrinology **is published monthly by The Endocrine Society (http://www.endo-society.org), the foremost professional society serving the endocrine community.**